IEEE Access
Multidisciplinary | Rapid Review | Open Access Journal

Received June 18, 2020, accepted August 10, 2020, date of publication August 25, 2020, date of current version September 4, 2020.

Digital Object Identifier 10.1109/ACCESS.2020.3019429

A Time Delay Estimation Based Adaptive Sliding Mode Strategy for Hybrid Impedance Control

MADAN MOHAN RAYGURU, MOHAN RAJESH ELARA, BRAULIO FÉLIX GÓMEZ, AND BALAKRISHNAN RAMALINGAM

Engineering Product Development, Singapore University of Technology and Design, Singapore 487372

Corresponding author: Madan Mohan Rayguru (mmrayguru87@gmail.com)

This work was supported in part by the National Robotics Programme under its Robotics Enabling Capabilities and Technologies under Grant 192 25 00051, in part by the National Robotics Programme under its Robot Domain Specific under Grant 192 22 00058, and in part by the Agency for Science, Technology and Research.

ABSTRACT This paper is inspired by the automation of cleaning tasks required inside the endogenous environment. This work intends to develop a robust adaptive strategy for force-position control, using robotic manipulators. With this objective, the operational/task space is decoupled into two sub-spaces, and the impedance model for the manipulator is designed using the standard second-order filters. The impedance filter generates the reference commands for the inner loop, which assures bounded position and force tracking. A delay estimation based adaptive sliding mode strategy is proposed for carrying out the tracking objective, and its convergence is proved using the Lyapunov-Razumikhin theorem. The controller uses past data to estimate the uncertainties in the error dynamics and exploits the sliding mode strategy to provide robustness in the closed-loop. This technique circumvents the under/overestimation issues, and linear/nonlinear parametrization requirements in conventional adaptive schemes. Multiple numerical simulations and experiments are performed, and the results point to the validity of the proposed control law in real-world settings.

INDEX TERMS Hybrid impedance control, automation of cleaning, time delay based adaptive control, robot manipulator.

I. INTRODUCTION

The indoor cleaning tasks for public places like community centers, hospitals, apartments have become increasingly critical in present-day scenarios. The recent pandemic also emphasizes the need for proper sanitation and maintenance of all indoor setups, which are frequently coming in contact with the people. The human operators generally carry these tasks, and there is a need to automate the cleaning tasks for better safety and frequency of operations.

Automating cleaning tasks has been the focus of the robotic researchers for a while now [1]. Air-duct cleaning by moving platforms has attracted much attention due to its complexities and challenges [2]. The authors of the paper [3] developed a new technique for aircraft-canopy polishing. The cleaning of household items is generally carried out using human service robots (HSR) [4]. The paper [5] presented a new strategy for automating can front cleaning. Similarly, automatic wiping and polishing tasks have been discussed in [6].

The above tasks require not only following a desired motion in the task space but also need to exert a predefined force for wiping/polishing surfaces [7]. In other words, a robot that is designed to automate these tasks should be able to simultaneously control the position of the end-effector and the force applied on the cleaning surface. As these tasks require the end-effector to remain in contact with the concerned environment, the end-effector movement is constrained (can not move freely in all directions) [8]. Similarly, the applied force should be in specific desired directions, and should not deviate much from the desired range [8].

The constrained manipulation of the robotic arm is carried out by selecting the suitable transformation from joint space to task space and formulating the Jacobian matrix for forward/inverse kinematics. A number of literature [9], discuss the stable manipulation using the robust control [10]–[12], adaptive control [13], [14], and model predictive control [15] techniques. Similarly, many force control techniques [16]

The associate editor coordinating the review of this manuscript and approving it for publication was Luigi Biagiotti.

FIGURE 1. Toyota HSR used for cleaning.

have been proposed to carry out grinding, wiping, and polishing tasks. The cleaning tasks generally requires the end-effector module to perform the repetitive motion, while simultaneously applying some desired force. So, controlling only the position or force will not lead to efficient cleaning performance.

In the seminal paper, the author of [17] proposed to decouple the motion and force control by suitably modeling the operational space. This strategy is called force-position control and has been successfully applied in completing various tasks [18]. In this method, the overall task space is divided into two decoupled spaces for manipulator movement and exerting force on the environment [19]. This idea is extended to the selection of different joints for movement and applying force, which circumvents various complications [20].

The force-position control technique does not consider the effect of environmental force on the manipulator velocity, which is natural in human hand movements [21]. Hence, the method does not generally apply for the situations where the motion direction and force direction are not decoupled [16], [18], [20]. The author of [21] proposed the celebrated impedance control strategy to mimic the human hand type motion on the robotic arms. The impedance control methodology defines the desired stiffness, damping of the robotic arm through carefully selected transfer functions, and then derive the control law such that the manipulator dynamics converge to the desired second-order impedance dynamics [22].

The authors of [23] developed a new strategy called hybrid impedance control (HIC) methodology to exploit the advantages of both force-position and impedance control techniques. The HIC technique divides the task space into two decoupled subspaces, which are then used for impedance control in two separate directions [23]. In general, the HIC requires a proper choice of decoupling matrix and impedance parameters (stiffness, damping) for better performance. Once this issue is sorted, the joint torques can be derived by using the large pool of robust and adaptive control techniques available in the literature [18], [24]–[27].

This work intends to focus on automating the indoor cleaning tasks, comprising of planar surfaces. The cleaning area may be a flat surface, an inclined plane [3], [5], or a dynamic moving plane like an escalator. The dynamic environment not only makes the friction force to vary but also make the force measurement inaccurate. Therefore, a conventional HIC may not assure satisfactory performance in such a setting. The adaptive strategies for HIC [25], [26] have issues with fast varying disturbances like contact forces. The sliding mode HIC [28] may have a chattering problem if proper care is not taken during implementation. Adaptive sliding mode technique may solve these issues but suffers from over/underestimation where the controller gains may shoot up or down near sliding surface [27]. This paper proposes a time delay estimation based adaptive sliding mode HIC scheme for this purpose. The proposed technique does not require the manipulator's parameters to be known and robust to environmental uncertainties. Unlike the traditional adaptive HIC strategies [25], [26], the force measurements and impedance parameters are used for generating the feed-forward part of the control law. In contrast, the feedback part compensates for any uncertainties in the feed-forward part, and system dynamics.

II. MATHEMATICAL MODEL & CONTROL OBJECTIVE

The cleaning task is generally performed by the robotic manipulators, and the attached cleaning modules. The mathematical model for the robotic hand of any arbitrary DOF in the joint space, can be written in the form of an Euler-Lagrangian dynamics, i.e:

$$M_j(q)\ddot{q} + C_j(q,\dot{q})\dot{q} + F_j(q,\dot{q}) + G_j(q) + J(q)^T F_e = \tau_j \quad (1)$$

where $q \in R^n$ is the joint state vector for the n-DOF manipulator. $M_j(.)$, $C_j(.)$, $G_j(.)$ and $F_j(.)$ represent inertia matrix, Coriolis matrix, Gravitational torque component, and friction component respectively. The matrix $J(.)$ is the manipulator Jacobian, τ_j is torque input to the joints, and F_e is the forces arising due to contact with the external environment.

The manipulator Jacobian maps the end-effector's position ($x \in R^m$) in the task/operational space to the joint space $q \in R^n$. In general $n \geq m$ for redundant manipulators, and $m = n$ for non redundant cases. Assuming the robot arm to be non redundant, the dynamics of the end effector in the task space can be expressed as:

$$M_t(q)\ddot{x} + C_t(q,\dot{q})\dot{x} + F_t(q,\dot{q}) + G_t(q) + F_e = \tau_e \quad (2)$$

where $M_t(.) = J^{-T}(.)M_j(.)J^{-1}$, $G_t(.) = J^{-T}(.)G_j(.)$, $F_t(.) = J^{-T}(.)F_j(.)$, $C_t(.) = J^{-T}(.)C_j(.)J^{-1} - J^{-T}(.)M_j(.)J^{-1}\dot{J}(.)J^{-1}(.)$, and $\tau_e = J^{-T}(.)\tau_j$.

A. IMPEDANCE CONTROL GOAL

The controller should be designed such that the joint torque τ_e delivered assure simultaneous position and force tracking with desired dynamic effects. So, the control task space is categorized into two decoupled sub-spaces which would describe force control, and position control directions. Let's define the two decoupled subspace as: $x = [x_p,\ x_f]$, where x_p is the part of task space used for position control and x_f is the part used for force control. The desired dynamics to be imparted on these directions are defined by the following second order differential equation.

$$M_d(\ddot{x} - \Sigma\ddot{x}_d) + B_d(\dot{x}_p - \Sigma\dot{x}_d) + K_d\Sigma(x_p - x_d) - (I - \Sigma)F_d = -F_e \quad (3)$$

where x_d is the desired trajectory along the position control, the matrices M_d, B_d, K_d, denote desired inertia, damping and stiffness in the control directions, and F_d is the desired force need to be impacted. To decouple the force and position control directions, a diagonal matrix Σ is chosen, consisting of ones and zeros. The ones represent the required position control directions. The dynamics (3) represents the desired impedance of the manipulator in contact with the environment.

The impedance control scheme is originally designed such that the robot should follow the dynamics of a second-order spring mass damper system. So, (3) describes a 2nd order differential equation with the design parameters M_d, B_d, K_d, Σ. As the cleaning surface is assumed flat, the parameter K_d is set to zero in force controlled direction, when in contact. This assures a proper steady-state force tracking. In other words, the desired impedance in force direction mimics a mass-dash pot system.

A moving surface can give rise to a varying external force, so the variable F_e is modeled as:

$$F_e = K_e(x - x_e) + B_e(\dot{x})$$

where x_e is the equilibrium position of the environment and K_e, B_e define stiffness, damping due to the environment, respectively. It should be noted that both K_e and B_e may vary due to the motion of the cleaning surface (in case of an escalator). So, an approximate value for them can be selected [23], [24], and the control law should be designed for compensating the inaccuracies.

One important aspect of impedance design is to ensure that the motion is controllable (not oscillating) while the manipulator loses contact. When the manipulator is free ($F_e = 0$), and the desired force F_d is constant, the impedance dynamics ($K_d = 0$) becomes [24],

$$M_d\ddot{x} + B_d\dot{x} = F_d.$$

So the transient part of the velocity is decided by $\frac{B_d}{M_d}$, whereas $\frac{F_d}{B_d}$ can bound the maximum velocity. So, a suitable choice of M_d and B_d can ensure controllable velocity in the absence of contact, irrespective of reference position trajectory, and distance from the environment.

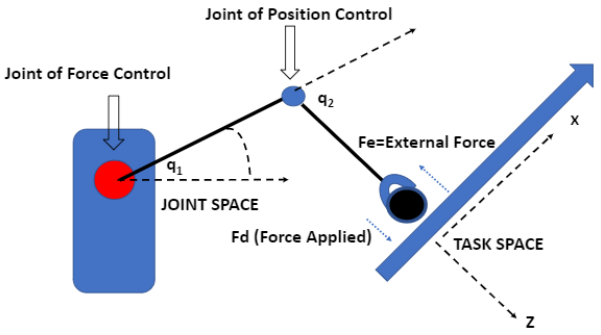

FIGURE 2. Schematic of a cleaning task using robotic Arm.

III. CONTROL LAW FORMULATION

Desired acceleration for the manipulator can be derived from (3) as:

$$a_d^o = M_d^{-1}\{-B_d(\dot{x} - \Sigma\dot{x}_d) - K_d\Sigma(x - x_d) + (I - \Sigma)F_d - F_e\} + \Sigma\ddot{x}_d. \quad (4)$$

Similarly, the desired velocity and position from (4) can be expressed as:

$$v_d^o = \int a_d^o\, dt, \quad p_d^o = \int v_d^o\, dt. \quad (5)$$

By inverse dynamics cancellation approach, the force required by the manipulator to track the desired acceleration a_d is given by

$$\tau_e = M_t(.)a_d^o + C_t(.)\int a_d^o + F_t(.) + G_t(.) + F_e. \quad (6)$$

However, the system dynamics is generally unknown, and therefore one needs to take account of the uncertainties while developing a control law.

A. DELAY BASED ADAPTIVE ROBUST DESIGN

Due to possible variation in F_e (in case of dynamic), the desired acceleration and velocity are changed to

$$a_d = a_d^o + \delta a_d, v_d = v_d + \delta v_d$$

Rewrite (2) as:

$$M_t(q)\ddot{x} + S_n = \tau_e \quad (7)$$

where the uncertain parts are combined into the term

$$S_n = C_t(.)\dot{x} + F_t(.) + G_t(.). - M_t(.)\delta a_d^o - C_t\delta v_d^o$$

As the system matrices in (7) are unknown, let's choose a control law

$$\tau_e = \hat{M}u_c + \hat{S}_n \quad (8)$$

where $\hat{S}_n$ is the estimate of S_n, u_c is the combination of feedforward and robust component of the control law. The matrix $\hat{M}$ is chosen as a constant diagonal matrix satisfying

$$||M_t^{-1}(.)\hat{M} - I|| < 1. \quad (9)$$

The desired acceleration a_d may contain some disturbances in force measurement F_e, so the term u_c is selected as the combination of a feedforward component u_f and robust component u_r(to be decided later). The feedforward component is selected as

$$u_c = u_f + u_r, \quad u_f = a_d^o + k_d(v_d^o - \dot{x}) + k_p(p_d^o - x), \quad (10)$$

where k_d, k_p are two positive definite matrices. This paper differs from the conventional adaptive hybrid impedance literature in the sense that, the estimate $\hat{S}_n$ is derived using time delay estimation approach [29]. The estimate is derived as:

$$\hat{S}_n = \tau_e^l - \hat{M}a_d^l \quad (11)$$

where τ_e^l and a_d^l denote the time delayed (by a small delay l) version of τ_e, a_d^o. Using the delayed version of the estimate, the closed loop is converted into:

$$\hat{M}a_d + \bar{S}_n = \tau_e^l \quad (12)$$

where

$$\bar{S}_n = (M_t(.) - \hat{M})a_v + \hat{M}a_d^l + S_n(.) - \hat{M}u_c$$

.

Define an error vector $E = [e^T, \dot{e}^T]^T$, where $e = p_d - x$ and $\dot{e} = v_d - \dot{x}$. Expanding τ_e^l, the closed loop dynamics (12) can be expressed as:

$$\dot{E} = A_1E + A_2E_l + B_oS_c - B_ou_r^l \quad (13)$$

where u_r^l is delayed version of u_r,

$$A_1 = \begin{bmatrix} 0 & I \\ 0 & 0 \end{bmatrix}, \quad A_2 = \begin{bmatrix} 0 & 0 \\ -k_d & -k_p \end{bmatrix}, \; B_o = \begin{bmatrix} 0 \\ I \end{bmatrix},$$
$$S_c = a_d^o - a_d^l + \hat{M}^{-1}(\bar{S}_n - \hat{S}_n^l).$$

The term S_c is the error due to time delay estimation. As,

$$E_l = E - \int_{-l}^{0} \dot{E}(t+r)dr$$

the equation (13) can be written as:

$$\dot{E} = A_oE + A_2E_l + B_o(S_c - u_r^l) - A_2\int_{-l}^{0} \dot{E}(t+r)dr \quad (14)$$

where $A_o = A_1 + A_2$. It should be noted that the matrix A_o can be made Hurwitz by proper selection of k_d and k_e. Hence, there exist a set of positive definite symmetric matrices P_o, Q_o such that

$$A_o^TP_o + P_oA_o = -Q_o.$$

To select the robust component of the control law, which would negotiate the time delay error S_c. Define a sliding surface $\xi = B_o^TP_oE$, and select an adaptive switching law as:

$$u_r = k_r(\alpha_1 + \alpha_2 + \alpha_3)\tanh(\xi),$$
$$\dot{\alpha}_1 = \begin{Bmatrix} k1||\xi|| \\ -k2||\xi|| \end{Bmatrix}$$
$$\text{if } \begin{Bmatrix} \alpha_1 \le \alpha_1^m \text{ or } (\xi\dot{\xi} > 0 \bigwedge \alpha_3 > \alpha_3^m \bigwedge \alpha_2 > \alpha_2^m) \\ \xi\dot{x}i \le 0 \bigwedge \alpha_3 \le \alpha_3^m \bigwedge \alpha_2 \le \alpha_2^m \end{Bmatrix}$$
$$\dot{\alpha}_3 = -\begin{Bmatrix} \frac{||\xi||}{\alpha_3} \\ 0 \end{Bmatrix} \text{ when } \begin{Bmatrix} \alpha_3 > \alpha_3^m \\ \alpha_3 \le \alpha_3^m \end{Bmatrix},$$
$$\dot{\alpha}_2 = -\begin{Bmatrix} \frac{1}{\alpha_2} \\ 0 \end{Bmatrix} \text{ when } \begin{Bmatrix} \alpha_2 > \alpha_2^m \\ \alpha_2 \le \alpha_2^m \end{Bmatrix} \quad (15)$$

where $k_r, k_1, k_2, \alpha_1^m, \alpha_2^m, \alpha_3^m \in R^+$, and $k_r > 1$. The initial conditions for the update of control gains $\alpha_1, \alpha_2, \alpha_3$ should be chosen as:

$$\alpha_1(0) > \alpha_1^m, \; \alpha_2(0) > \alpha_2^m, \; \alpha_3(0) > \alpha_3^m.$$

The adaptive sliding mode control law given in (15), can be made continuous with a small tweak as: $u_r = k_r(\alpha_1 + \alpha_2 + \alpha_3)\tanh(\xi)$ if $(||\xi|| > \mu)$ and $u_r = k_r(\alpha_1 + \alpha_2 + \alpha_3)\frac{\xi}{\mu}$ otherwise.

Analytic Comparison: By combining all the uncertainties in the term S_n, the delay based estimation scheme compensate for uncertainties arising from both system model, and variation in the cleaning surface. The unknown external forces and varying frictional forces may not be linearly parametrized, so a conventional adaptive strategy may not work. A neural network-based scheme may also be useful in such cases, but the number of internal nodes and the type of activation function must be appropriately chosen. It should be noted that the proposed controller does not need any regressor matrix, and need to adapt only three gain parameters $\alpha_1, \alpha_2, \alpha_3$. Moreover, the controller does not suffer from under-estimation and over-estimation problem, unlike conventional adaptive designs.

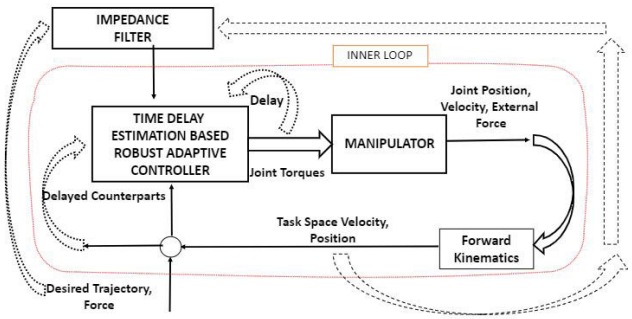

FIGURE 3. Block diagram of the proposed controller.

IV. CONVERGENCE OF TRACKING ERROR

The overall control law (8) consists of a feedforward part (10) and robust part (15), along with the delay based estimation part (11). The closed loop system in the joint space is derived as (14). The convergence analysis of (14) exploits sliding mode technique and Razumikhin's theorem for the fulfillment of the objective.

Note: The Razumikhin theorem [27], provide a delay independent stability analysis framework for time-delay systems. As the closed loop dynamics (14) has both state delay and input delay, we need to exploit the theorem

for convergence analysis. For a Lyapunov function V(x(t)), the Razumikhin theorem points to the existence of a positive scalar ν such that

$$V(x(t_1)) < \nu V(x(t))$$

for all $t - 2l \leq t_1 \leq t$, where l is a finite time delay.

It should be noted that the closed loop dynamics can only be made stable by Razumikhin technique if the time delay error term S_c is bounded [27]. By ensuring the condition (9), the error S_c can be made upper bounded by a positive scalar [29], even though the constant is unknown, i.e.:

$$||S_c|| \leq \bar{\alpha}_1$$

where $\bar{\alpha}_1 \in R^+$ and unknown.

As already suggested, the constant $\bar{\alpha}_1$ is unknown, and the robust part of the control law u_r tries to nullify it's effect. In this direction, define a composite Lyapunov function

$$V = V_1 + \frac{1}{2}(\alpha_1 - \bar{\alpha}_1)^2 + \frac{1}{2}\Upsilon_1\alpha_2^2 + \frac{1}{2}\Upsilon_2\alpha_3^2 \quad (16)$$

where $V_1 = \frac{1}{2}E^T P_o E$, and Υ_1, Υ_2 are two positive constants defined later. The Razumikhin's theorem for V, can be expressed as:

$$\begin{aligned} &V(E(t_1), \alpha_1(t_1), \alpha_2(t_1), \alpha_3(t_1)) \\ &\quad < \nu V(E(t), \alpha_1(t), \alpha_2(t), \alpha_3(t)) \\ &\quad \Rightarrow E^T(t_1)P_oE(t_1) < \nu E^T(t)P_oE(t) + \theta(t_1) \end{aligned} \quad (17)$$

where

$$\begin{aligned} \theta(t_1) = \nu\{&\frac{1}{k1}((\alpha_1(t_1) - \bar{\alpha}_1)^2 - (\alpha_1(t) - \bar{\alpha}_1)^2) \\ &+ \Upsilon_1(\alpha_2^2(t_1) - \alpha_2^2(t)) + \Upsilon_2(\alpha_3^2(t_1) - \alpha_3^2(t))\}. \end{aligned} \quad (18)$$

The time derivative of V along (14) can be expressed as:

$$\begin{aligned} \dot{V} = -\frac{1}{2}E^T Q_o E + \xi^T H(t) - \int_{-l}^{0} E^T P_o A_2 \{&A_1 E(t+r) \\ &+ A_2 E(t+r-l) + B_o H(t+r)\}dr \end{aligned} \quad (19)$$

where $H(t) = S_c - u_r^l$. The last term inside the integral can be simplified as:

$$\begin{aligned} \int_{-l}^{0} \{&E^T P_o A_2 A_1 E(t+r) + E^T P_o A_2 A_2 E(t+r-l) \\ &+ E^T P_o A_2 B_o H(t+r)\}dr. \end{aligned}$$

Using Razumikhin's theorem and few simple matrix manipulation:

$$\begin{aligned} -\int_{-l}^{0} \{E^T P_o A_2 A_1 E(t+r)\}dr &\leq \frac{1}{2}\{\frac{l\nu}{\kappa}E^T P_o E \\ &+ l\kappa E^T (P_o A_2 A_1 P_o^{-1} A_1^T A_2^T P_o)E + \frac{1}{\kappa}\int_{-l}^{0}\theta(t+r)dr\} \\ -\int_{-l}^{0} \{E^T P_o A_2 A_2 E(t+r-l)\}dr &\leq \frac{1}{2}\{\frac{l\nu}{\kappa}E^T P_o E \\ &+ l\kappa E^T (P_o A_2 A_2 P_o^{-1} A_2^T A_2^T P_o)E + \frac{1}{\kappa}\int_{-l}^{0}\theta(t+r-l)dr\} \\ -\int_{-l}^{0} \{E^T P_o A_2 B_o H(t+r)\}dr &\leq \frac{1}{2}\{l\kappa E^T (P_o A_2 P_o^{-1} A_2^T P_o)E \\ &+ \frac{1}{\kappa}\int_{-l}^{0}(H^T(t+r)B_o^T P_o B_o H(t+r))dr\} \end{aligned}$$

Using these simplifications, the time derivative of V, can be expressed as:

$$\dot{V} \leq -\frac{1}{2}E^T(Q_o - l\Gamma)E + \xi^T(S_c - u_r) + \Upsilon_1 + \Upsilon_2||\xi|| \quad (20)$$

where

$$\Gamma = \frac{2\nu}{\kappa}P_o + \nu P_o A_2(P_o^{-1} + A_1 P_o^{-1} A_1^T + A_2 P_o^{-1} A_2^T)A_2^T P_o \quad (21)$$

The constant Υ_1, Υ_2 are derived using Lipschitz properties, i.e:

$$||u_r - u_r^l|| \leq \Upsilon_2 \quad (22)$$

$$\begin{aligned} \frac{1}{2\kappa}\Big|\Big| \int_{-l}^{0} \{&(H^T(t+r)B_o^T P_o B_o H(t+r)) \\ &+ \theta(t+r) + \theta(t+r-l)\}dr\Big|\Big| \leq \Upsilon_1 \end{aligned} \quad (23)$$

Proposition 1: The closed loop system (14) is stable, only if the time-delay l satisfies:

$$l < \frac{\lambda_{min}(Q_o)}{||\Gamma||} \quad (24)$$

Proof: The dynamics (14) can be stable, if the first term in R.H.S of equation (20) is negative definite. For that to happen,

$$(Q_o - l\Gamma) > 0 \Rightarrow l < \frac{\lambda_{min}(Q_o)}{||\Gamma||}. \odot$$

Exploiting (15), (11), and (8) on (20), the Lyapunov stability analysis can be carried out further. Let's consider the scenario when

$$\alpha_1 \leq \alpha_1^m \text{ or } (\xi\dot{\xi} > 0 \wedge \alpha_3 > \alpha_3^m \wedge \alpha_2 > \alpha_2^m).$$

Exploiting (15) for this scenario, (20) can be rewritten as:

$$\begin{aligned} \dot{V} \leq -\frac{E^T(Q_o - l\Gamma)E}{2} + \Upsilon_1 + \Upsilon_2||\xi|| + \Upsilon_1\alpha_2\dot{\alpha}_2 + \Upsilon_2\alpha_3\dot{\alpha}_3 \\ + \xi^T(S_c - k_r(\alpha_1 + \alpha_2 + \alpha_3)\tanh(\xi)) + (\alpha_1 - \bar{\alpha}_1)||\xi|| \end{aligned}$$

From (15),

$$\begin{aligned} \dot{V} \leq -\frac{E^T(Q_o - l\Gamma)E}{2} + +\bar{\alpha}_1||\xi|| \\ - k_r(\alpha_1 + \alpha_2 + \alpha_3)||\xi|| + (\alpha_1 - \bar{\alpha}_1)||\xi|| \end{aligned}$$

As $k_r > 1$,

$$\dot{V} \leq -\frac{E^T(Q_o - l\Gamma)E}{2} \leq -\frac{\lambda_{min}(Q_o - l\Gamma)}{2}||E||^2$$

Hence, by exploiting Barbalat's lemma [29], we get

$$\lim_{t\to\infty}\dot{V} = 0 \Rightarrow \lim_{t\to\infty} E = 0$$

Now consider the opposite scenario, for which the term $\dot{V}$ can written as:

$$\dot{V} \leq -\frac{E^T(Q_o - l\Gamma)E}{2} + \Upsilon_1 + \Upsilon_2||\xi|| + \Upsilon_1\alpha_2\dot{\alpha}_2 + \Upsilon_2\alpha_3\dot{\alpha}_3 + \xi^T(S_c - k_r(\alpha_1+\alpha_2+\alpha_3)\tanh(\xi)) - \frac{k2}{k1}(\alpha_1 - \bar{\alpha}_1)||\xi||$$

Exploiting (15), and the fact that $||\xi|| \leq ||B_o^T P_o||||E||$, one can derive

$$\dot{V} \leq -\frac{\lambda_{min}(Q_o - l\Gamma)}{2}||E||^2 + \Upsilon_1 + \Upsilon_2||B_o^T P_o||||E|| + 2\frac{k2}{k1}\bar{\alpha}_1||B_o^T P_o||||E||$$

Hence, the closed loop system is assured to be uniformly ultimately bounded (UUB), with a bound

$$B_n = b_n + \sqrt{b_n^2 + \frac{2\Upsilon}{\lambda_{min}(Q_o - l\Gamma)}}$$

$$b_n = \frac{\Upsilon_2 + 2\frac{k2}{k1}\bar{\alpha}_1}{\lambda_{min}(Q_o - l\Gamma)}||B_o^T P_o||$$

The closed loop steady state error B_n can be made arbitrary small by selecting a small delay and a larger Q_o. Generally, the delay can be chosen as small as the sampling time for better accuracy. The above analysis can be summarized as the following theorem.

Theorem 1: Let proposition 1 holds true. If a control law is chosen as given in (8), (11) and (15) in the task space, then the unknown manipulator dynamics asymptotically converge to the described impedance dynamics (2). ⊙

NOTE: The theorem assures bounded tracking, provided the delay is bounded by the condition (24). However, the amount of delay directly affects the steady-state error (B_n, b_n in UUB condition), and the sampling interval restricts the minimum delay. As the sampling has to be faster to get a smaller steady-state error, there exists a trade-off between condition (24) and small, steady-state error.

The design parameter α_1 in (15) can be used to modify the robustness against the estimation error due to time delay. Similarly, the parameters α_2 and α_3 can be used to alter the closed-loop performance/stability. Other design scalars like $k_r, \alpha_1^m, \alpha_2^m, \alpha_3^m$ may be tuned by trial and error

V. SIMULATION

A two-link manipulator is used for simulation, whose parameters are $m_1 = 10\ kg, m_2 = 5kg, l_1 = 0.2m, l_2 = 0.1m, g = 9.81m/s^2$. The system matrices are given by:

$$M_j = \begin{bmatrix} M_1 & M_2 \\ M_2 & M_3 \end{bmatrix}, \quad F_j = \begin{bmatrix} 0.5\ sgn(\dot{q}_1) \\ 0.5\ sgn(\dot{q}_2). \end{bmatrix}$$

$$M_1 = (m_1 + m_2)l_1^2 + m_2\ l_2(l_2 + 2l_1\cos(q_2))$$

$$M_2 = m_2\ l_2(l_2 + l_1\cos(q_2)), M_3 = m_2\ l_2^2$$

$$M_j = \begin{bmatrix} C_1 & C_2 \\ 0 & C_3 \end{bmatrix}, \quad G_j = \begin{bmatrix} G_1 \\ G_2. \end{bmatrix}$$

$$C_1 = -m_2\ l_1\ l_2\sin(q_2)\dot{q}_2, \quad C_2 = C_1 - m_2\ l_1\ l_2\sin(q_2)\dot{q}_1,$$

$$C_3 = -C_1, \quad G_2 = m_2 g l_2\cos(q_1 + q_2)$$

$$G_1 = G_1 + m_1 g l_1\cos(q_1) + m_2 g l_1\cos(q_1).$$

The Jacobian matrix is given by:

$$J = \begin{bmatrix} \sin(q_1) + \sin(q_1 + q_2) & \sin(q_1 + q_2) \\ \cos(q_1 + q_2) & \cos(q_1 + q_2) + \cos(q_1) \end{bmatrix}.$$

The impedance parameters are selected as:

$$M_d = diag([3, 6]), \quad B_d = diag([30, 60]),$$
$$K_d = diag([250, 0]).$$

The external force is modeled using:

$$K_e = diag([0, 180N/m]), \quad B_e = diag([0, 80\ N.sec/m]).$$

To model the variation in the external force due to movement of handrail a disturbance signal $0.2\sin(0.5t)N$ is added to f_e. The desired force to be exerted is taken as $F_d = 3.5\ N$, where as the desired trajectory in position controlled direction is taken as $x_d = 0.3\sin(t)m$.

For realizing the controller the following parameters are chosen:

$$\hat{M}_t = 0.05I, \quad k_d = -30,\ k_p = -150.$$

For this choice of $\hat{M}$, the condition for bounded time delay estimation error can be satisfied, and the control gains k_p, k_d, with the matrix $Q_o = I$, gives rise to

$$P_o = \begin{bmatrix} 0.1168 & -0.5000 \\ -0.5000 & 2.5167 \end{bmatrix}.$$

Choosing the sampling time equal to the delay $l = 0.001\ sec$, the constants $\nu = 1.006, \kappa = 0.08$ satisfy the delay time requirement in proposition 1. The gain parameters of u_r are chosen as $\bar{\alpha}_1 = 0.005, \alpha_2^m = \alpha_3^m = 0.5$, where as other parameters are chosen by trial and error.

The closed loop simulations are carried out without any external disturbances are presented in figure 4-8. Figure 4 shows the position tracking along x-direction, whereas figure 5 shows force tracking. The steady state error for the force tracking is very small, which can be further reduced by a smaller sampling time.

The evolution of the sliding surface shown in figure 6 points to some initial transient, which may arise due to large error at initial conditions. The adaptive gains shown in figure 7, 8 and 9 remain bounded for all time, which confirms our convergence analysis.

To show the impedance tracking abilities of the proposed controller, define the auxiliary error vector as

$$e_{aux} = M_d(\ddot{x} - \Sigma\ddot{x}_d) + B_d(\dot{x}_p - \Sigma\dot{x}_d) + K_d\Sigma(x_p - x_d) - (I - \Sigma)F_d + F_e \quad (25)$$

The figure 10 shows that $e_{aux} \rightarrow 0$ in position controlled direction and tends to a very small steady state value in force controlled direction. It confirms asymptotic impedance tracking ability of the proposed controller.

To validate the effectiveness of the proposed control law, the simulation is repeated with the added uncertainties in the

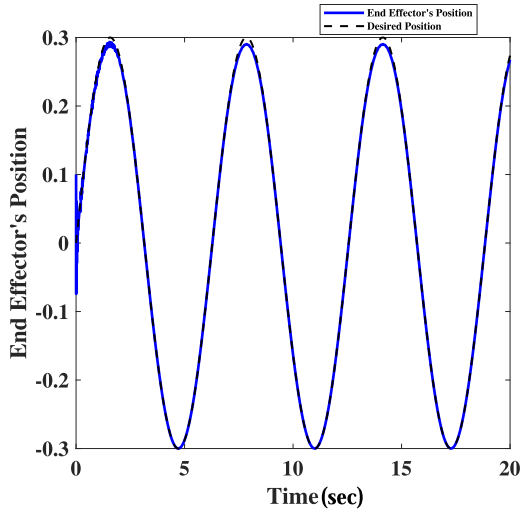

FIGURE 4. Position tracking in x direction without disturbance.

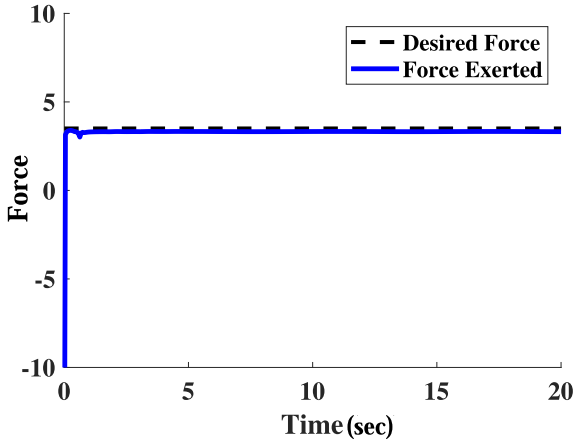

FIGURE 5. Force tracking in z direction without disturbance.

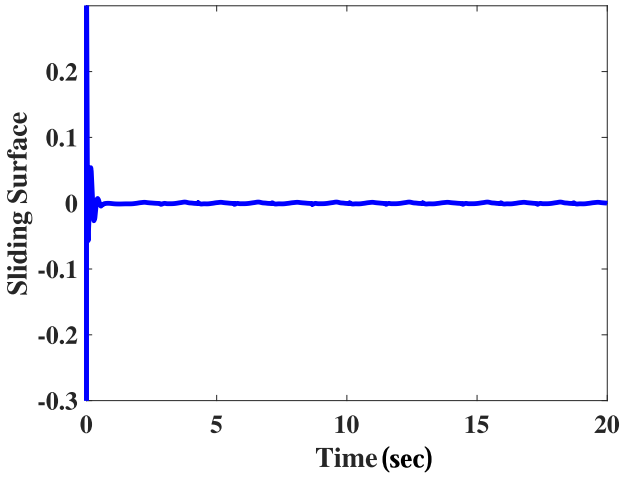

FIGURE 6. Sliding surface.

term F_e. The effect of the disturbance can be observed from the initial transient errors in position tracking (figure 11), and small oscillations in force tracking (figure 12), even though the error is small. By reducing the sampling interval, these errors can be further reduced.

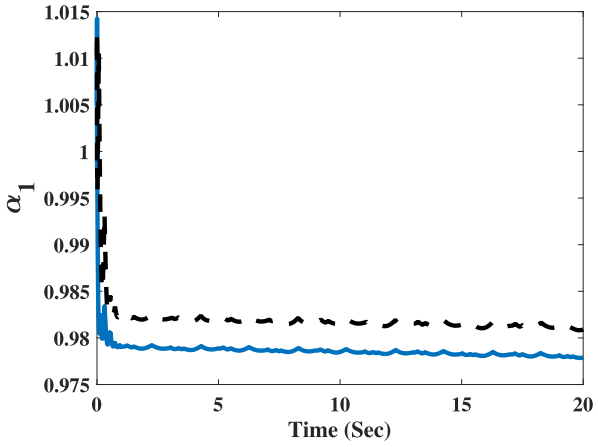

FIGURE 7. Estimation of control gain vector α_1.

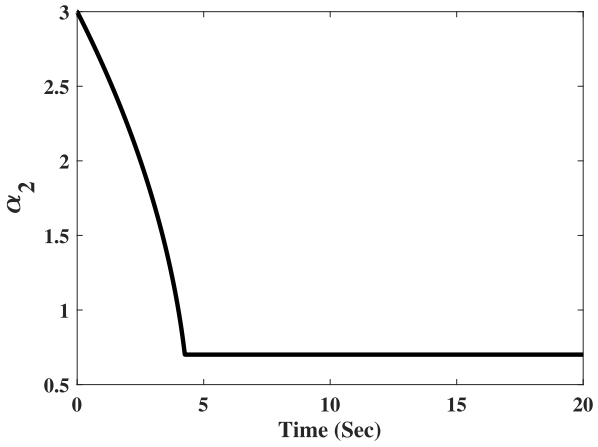

FIGURE 8. Estimation of control gains α_2.

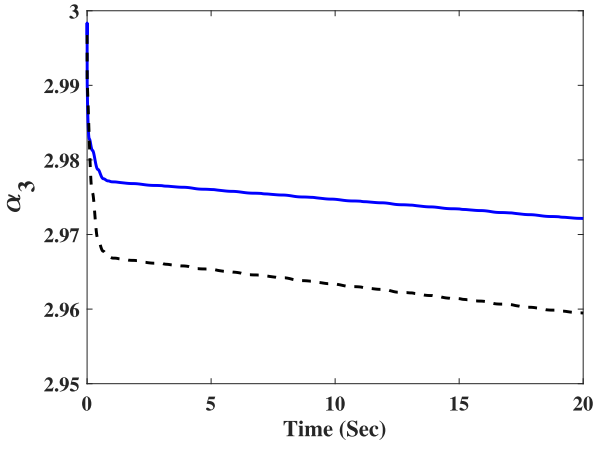

FIGURE 9. Estimation of control gains α_3.

VI. EXPERIMENTAL RESULTS

For implementation of the proposed controller, a Toyota HSR platform is chosen as the test-bed. The HSR is a position

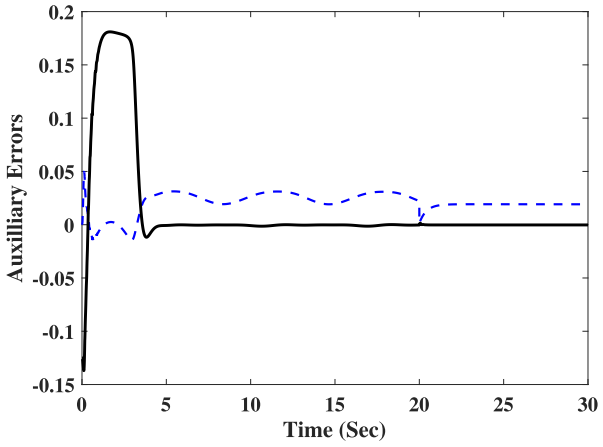

FIGURE 10. Auxiliary errors.

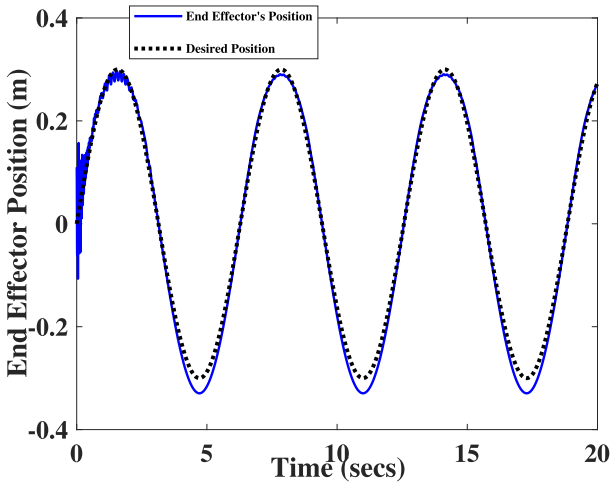

FIGURE 11. Position in x direction in the presence of uncertainties in external environment.

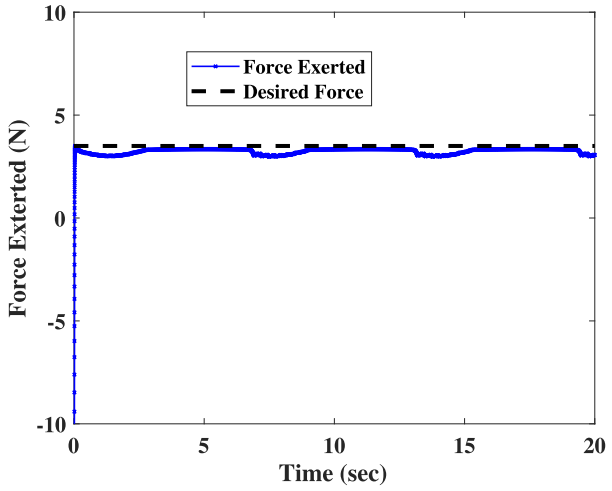

FIGURE 12. Force in z direction in the presence of uncertainties in external environment.

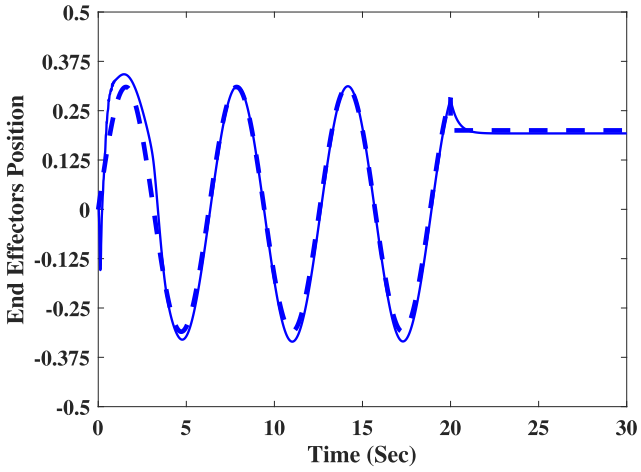

FIGURE 13. Tracking with change in desired trajectories and disturbance.

controlled robot, and therefore the torque command has to be transformed before implementation. We have used a simple torque-position transformation [30], which is given by

$$q_{ref}(k) = k_{ref}^{-1}\tau_c(k-1) + q(k-1) \tag{26}$$

where $q_{ref}(k)$ represents commanded position, k_{ref} is a positive constant, $\tau_c(k-1)$ is the torque sample from previous instant. Even though it is not an exact approach, it has been shown to work satisfactorily in the literature [30], [31]. The constant parameter k_{ref} is tuned by trial and error for a few known desired trajectory, before fixing it to $k_{ref} = 15$. The controller is implemented using python-ROS interface, and the sensor measurements are collected using ROS package. For all experiments, the sampling interval is chosen as 1 ms.

The HSR is manually moved near the handrail, and only two joints (arm flex and wrist flex) are activated for the experiment. Initially, the desired position is set as 0.3 $sin(t)m$ for 20 seconds, and changed to a constant value $0.25m$ after that. The response of the gripper position is plotted in figure 13. The small steady state error can be explained by the inaccuracies in the torque-position transformation.

The proposed controller is compared with a proportional derivative (PD) controller, conventional adaptive controller [25], [26] and a sliding mode controller [28]. The desired trajectory is set as 0.3 $sin(t)m$ for 20 secs, after which it is changed to 0.2 $sin(t)m$. The comparison results are presented in the following figures.

As the PD controller acts without any model knowledge, a comparatively inferior, trajectory and force tracking can be observed from the figure. It is observed that the steady-state trajectory tracking for the conventional adaptive and sliding mode impedance controller is similar to the proposed controller. However, both methods give rise to comparatively larger transient errors, both in trajectory and force tracking. The transient errors in the conventional adaptive controller are due to the comparatively slower adaptation to the desired trajectory changes and the sudden change in the impedance during initial contact. The sliding mode controller does not

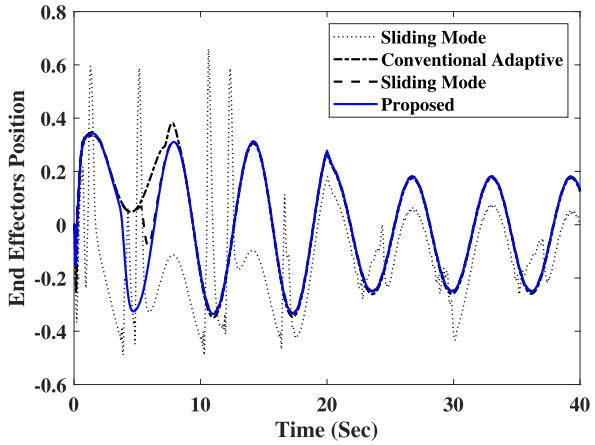

FIGURE 14. Comparison of tracking in position controlled subspace.

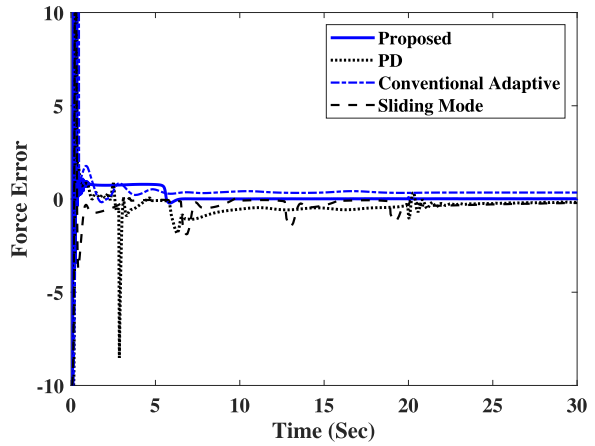

FIGURE 15. Comparison of force errors.

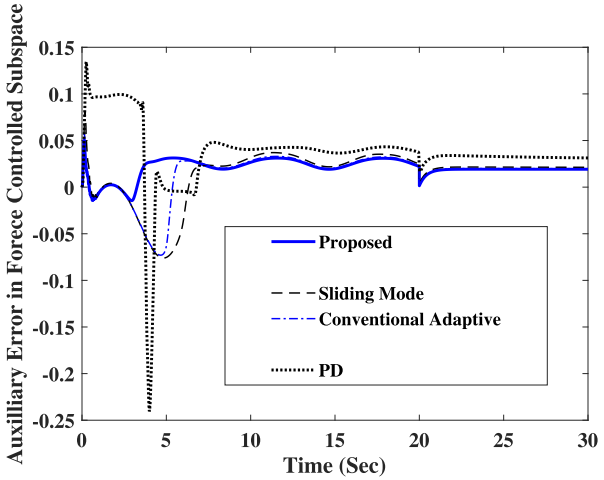

FIGURE 16. Comparison of Aux. Error in force controlled subspace.

suffer from slowness, but it suffers from discontinuity of the control law, whose effects can be observed as perturbations in the force tracking error. The proposed controller is not slow to adapt, does not suffer from chattering, and does not have over/underestimation issues. Hence, it has comparatively better performance in both the trajectory as well as force tracking. The initial transient errors for the proposed controller can be explained by the time delay based estimation technique, which comes to effect after a small initial time period. The effect can be suppressed by saturating the control law beyond the region of interest.

VII. CONCLUSION

A new strategy is proposed for hybrid impedance controller design using time delay estimation technique. The standard second order impedance filter is used to generate the reference trajectories for the inner loop. The control law comprises of a feed-forward segment and an adaptive sliding mode segment. The adaptation technique does not suffer from over/underestimation problems and does not need regressor matrix computation. The controller is suitable for cleaning handrails, escalators, and other plane surfaces, which is verified through numerical simulations and experiments.

ACKNOWLEDGEMENT

The authors would like to thank, the National Robotics Programme, the Agency for Science, Technology and Research, and SUTD for their support.

REFERENCES

[1] M. Vega-Heredia, R. E. Mohan, T. Y. Wen, J. S. 'Aisyah, A. Vengadesh, S. Ghanta, and S. Vinu, "Design and modelling of a modular window cleaning robot," *Autom. Construction*, vol. 103, pp. 268–278, Jul. 2019.
[2] B. Dexu, K. Weiwei, and Q. Yunlong, "A task-space tracking control approach for duct cleaning robot based on fuzzy wavelet neural network," *J. Dyn. Syst., Meas., Control*, vol. 141, no. 11, Nov. 2019, Art. no. 111004.
[3] R. Jamisola, M. H. Ang, D. Oetomo, O. Khatib, T. Ming Lim, and S. Yong Lim, "The operational space formulation implementation to aircraft canopy polishing using a mobile manipulator," in *Proc. IEEE Int. Conf. Robot. Autom.*, vol. 1, May 2002, pp. 400–405.
[4] T. Yamamoto, K. Terada, A. Ochiai, F. Saito, Y. Asahara, and K. Murase, "Development of human support robot as the research platform of a domestic mobile manipulator," *ROBOMECH J.*, vol. 6, no. 1, p. 4, Dec. 2019.
[5] J. Moura, W. Mccoll, G. Taykaldiranian, T. Tomiyama, and M. S. Erden, "Automation of train cab front cleaning with a robot manipulator," *IEEE Robot. Autom. Lett.*, vol. 3, no. 4, pp. 3058–3065, Oct. 2018.
[6] Q. Zhou and X. Li, "Experimental comparison of drag-wiper and roller-wiper glass-cleaning robots," *Ind. Robot: Int. J.*, vol. 43, no. 4, pp. 409–420, Jun. 2016.
[7] F. Nagata, T. Hase, Z. Haga, M. Omoto, and K. Watanabe, "CAD/CAM-based position/force controller for a mold polishing robot," *Mechatronics*, vol. 17, nos. 4–5, pp. 207–216, May 2007.
[8] J. K. Mills and A. A. Goldenberg, "Force and position control of manipulators during constrained motion tasks," *IEEE Trans. Robot. Autom.*, vol. 5, no. 1, pp. 30–46, Feb. 1989.
[9] L. Tian, J. Wang, and Z. Mao, "Constrained motion control of flexible robot manipulators based on recurrent neural networks," *IEEE Trans. Syst., Man Cybern., B (Cybern.)*, vol. 34, no. 3, pp. 1541–1552, Jun. 2004.
[10] K. D. Young, "Application of sliding mode to constrained robot motion control," in *Proc. Amer. Control Conf.*, Jun. 1988, pp. 912–918.
[11] M. M. Rayguru and I. N. Kar, "Contraction-based stabilisation of nonlinear singularly perturbed systems and application to high gain feedback," *Int. J. Control*, vol. 90, no. 8, pp. 1778–1792, Aug. 2017, doi: 10.1080/00207179.2016.1221139.
[12] M. M. Rayguru and I. N. Kar, "Contraction theory approach to disturbance observer based filtered backstepping design," *J. Dyn. Syst., Meas., Control*, vol. 141, no. 8, Aug. 2019, Art. no. 084501.
[13] C.-Y. Su, T. P. Leung, and Q.-J. Zhou, "Adaptive control of robot manipulators under constrained motion," in *Proc. 29th IEEE Conf. Decis. Control*, Dec. 1990, pp. 2650–2655.

[14] B. Yao and M. Tomizuka, "Adaptive control of robot manipulators in constrained motion: Controller design," *J. Dyn. Syst., Meas., Control*, vol. 117, no. 3, pp. 320–328, 1995.
[15] J. de Carufel and D. S. Necsulescu, "Model predictive control for impact-contact motion of a manipulator," in *Proc. Can. Conf. Electr. Comput. Eng.*, vol. 1, Sep. 1995, pp. 330–333.
[16] G. Zeng and A. Hemami, "An overview of robot force control," *Robotica*, vol. 15, no. 5, pp. 473–482, Sep. 1997.
[17] O. Khatib, "A unified approach for motion and force control of robot manipulators: The operational space formulation," *IEEE J. Robot. Autom.*, vol. 3, no. 1, pp. 43–53, Feb. 1987.
[18] V. Ortenzi, R. Stolkin, J. Kuo, and M. Mistry, "Hybrid motion/force control: A review," *Adv. Robot.*, vol. 31, nos. 19–20, pp. 1102–1113, Oct. 2017.
[19] M. Mistry and L. Righetti, "Operational space control of constrained and underactuated systems," in *Robotics: Science and Systems VII*. 2012, pp. 225–232.
[20] J. Nakanishi, R. Cory, M. Mistry, J. Peters, and S. Schaal, "Operational space control: A theoretical and empirical comparison," *Int. J. Robot. Res.*, vol. 27, no. 6, pp. 737–757, Jun. 2008.
[21] N. Hogan, "Impedance control: An approach to manipulation. I: Theory," *J. Dyn. Syst., Meas., Control*, vol. 107, no. 1, pp. 1–7, 1985.
[22] R. Kelly, R. Carelli, M. Amestegui, and R. Ortega, "On adaptive impedance control of robot manipulators," in *Proc. Int. Conf. Robot. Autom.*, May 1989, pp. 572–577.
[23] R. J. Anderson and M. W. Spong, "Hybrid impedance control of robotic manipulators," *IEEE J. Robot. Autom.*, vol. 4, no. 5, pp. 549–556, Mar./Apr. 1988.
[24] G. J. Liu and A. A. Goldenberg, "Robust hybrid impedance control of robot manipulators," in *Proc. IEEE Int. Conf. Robot. Autom.*, Apr. 1991, pp. 287–292.
[25] J. Li, L. Liu, Y. Wang, and W. Liang, "Adaptive hybrid impedance control of robot manipulators with robustness against environment's uncertainties," in *Proc. IEEE Int. Conf. Mechatronics Autom. (ICMA)*, Aug. 2015, pp. 1846–1851.
[26] M. Hosseinzadeh, P. Aghabalaie, H. A. Talebi, and M. Shafie, "Adaptive hybrid impedance control of robotic manipulators," in *Proc. 36th Annu. Conf. IEEE Ind. Electron. Soc. (IECON)*, Nov. 2010, pp. 1442–1446.
[27] S. Roy, I. N. Kar, J. Lee, and M. Jin, "Adaptive-robust time-delay control for a class of uncertain Euler–Lagrange systems," *IEEE Trans. Ind. Electron.*, vol. 64, no. 9, pp. 7109–7119, Sep. 2017.
[28] A. Hace, S. Uran, K. Jezernik, and B. Curk, "Robust sliding mode based impedance control," in *Proc. IEEE Int. Conf. Intell. Eng. Syst.*, Sep. 1997, pp. 77–82.
[29] S. Roy, S. Nandy, R. Ray, and S. N. Shome, "Robust path tracking control of nonholonomic wheeled mobile robot: Experimental validation," *Int. J. Control, Autom. Syst.*, vol. 13, no. 4, pp. 897–905, Aug. 2015.
[30] N. Adhikary and C. Mahanta, "Inverse dynamics based robust control method for position commanded servo actuators in robot manipulators," *Control Eng. Pract.*, vol. 66, pp. 146–155, Sep. 2017. [Online]. Available: http://www.sciencedirect.com/science/article/pii/S0967066117301521
[31] A. Del Prete, N. Mansard, O. E. Ramos, O. Stasse, and F. Nori, "Implementing torque control with high-ratio gear boxes and without joint-torque sensors," *Int. J. Humanoid Robot.*, vol. 13, no. 01, Mar. 2016, Art. no. 1550044, doi: 10.1142/S0219843615500449.

MADAN MOHAN RAYGURU received the B.Tech. degree from BPUT Odisha, India, the master's degree in electrical engineering from NIT Roukela, and the Ph.D. degree in control systems from the Indian Institute of Technology, Delhi, India. He is currently a Research Fellow with the Engineering Product Development Pillar, Singapore University of Technology and Design (SUTD). His research interests include robotics, convergent systems, and saturated controller design.

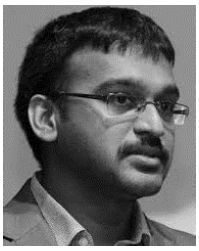

MOHAN RAJESH ELARA received the B.E. degree from the Amrita Institute of Technology and Sciences, Bharathiar University, India, and the M.Sc. degree in consumer electronics and the Ph.D. degree in electrical and electronics engineering from Nanyang Technological University, Singapore. He is currently an Assistant Professor with the Engineering Product Development Pillar, Singapore University of Technology and Design (SUTD). Before joining SUTD, he was a Lecturer with the School of Electrical and Electronics Engineering, Singapore Polytechnic. His research interests are in robotics with an emphasis on self-reconfigurable platforms as well as research problems related to robot ergonomics and autonomous systems. He has published more than 80 papers in leading journals, books, and conferences. He was a recipient of SG Mark Design Award, in 2016, 2017, and 2018, A' Design Award in 2018, ASEE Best of Design in Engineering Award, in 2012, and Tan Kah Kee Young Inventors' Award, in 2010. He has served in various positions of organizing and technical committees of over twenty international competitions and conferences. He is also a Visiting Faculty Member of the International Design Institute, Zhejiang University, China.

BRAULIO FÉLIX GÓMEZ received the bachelor's degree in informatics engineering from the Technological Institute of Los Mochis, México, and the technician degree in mechatronics from the Industrial Technological and Services Baccalaureate Center #43. He is currently a Research Fellow with the ROAR Lab, Singapore University of Technology and Design (SUTD).

BALAKRISHNAN RAMALINGAM received the B.Sc. and M.Sc. degrees in electronics from Bharathidasan University, Tiruchirapalli, India, in 2006 and 2009, respectively, and the Ph.D. degree in VLSI design from SASTRA University, Thanjavur, India. He is currently a Postdoctoral Research Fellow with the ROAR Lab, Singapore University of Technology and Design, Singapore. His research interests include artificial intelligence, computer vision, embedded system design, reconfigurable hardware, information security, and multiprocessor system on chip.